Solid-State and Surface Spectroscopic Characterization of $BaTiO_3$ Fine Powders

Guido Busca,*,† Vincenzo Buscaglia,‡ Marcello Leoni,‡ and Paolo Nanni†

Istituto di Chimica, Facoltà di Ingegneria, Università, P. le Kennedy, I-16129 Genova, Italy, and Istituto di Chimica Fisica Applicata dei Materiali, CNR, Area della Ricerca, via de Marini 6, I-16149 Genova, Italy

Received February 1, 1994. Revised Manuscript Received April 27, 1994®

The bulk and surface structure of two $BaTiO_3$ powders has been investigated by FT-IR and FT-Raman spectroscopies. A high-area sample (39 m^2/g), produced by a hydrothermal method, cubic to XRD, appears to have lower symmetry to Raman spectroscopy, with unit-cell distortions similar to those of tetragonal ferroelectric $BaTiO_3$. It contains $BaCO_3$ impurities, leading to a bulk Ba/Ti ratio lower than 1, as also evidenced by Raman spectra. Bulk hydroxy groups are evident, possibly needed to balance such a charge defect. Calcination at 1223 K causes the disappearance of these impurities and converts this material in the usual tetragonal phase. The surface properties of both powders, investigated through water and pyridine adsorption, are similar and appear to be dominated by Ba^{2+} ions, so leading to a solid characterized by extremely weak Lewis acidity. An interpretation for the solid-state behavior of the starting powder is proposed.

Introduction

$BaTiO_3$ is a well-known ferroelectric ceramic material applied in high-permettivity multilayer capacitors.[1] Other unusual characteristics of $BaTiO_3$ such as its photorefractive properties[2] and its positive temperature coefficient effect[3] have also been the object of recent investigation.

The preparation of ceramics in a highly dispersed form, as in the case of sol–gel and hydrothermal preparations, is useful in order to obtain, by successive sintering, bulk materials with superior microstructure. From this point of view, the knowledge of the surface structure of high area ceramic powders can be useful to understand their behavior with respect to sintering.[4] Moreover, in the particular case of $BaTiO_3$ the investigation of small particle preparations is of interest in relation to the great influence of particle size on its dielectric and ferroelectric properties.[5,6] In fact, it has been reported that the paraelectric–ferroelectric phase transition vanishes when the particle (grain) size of $BaTiO_3$ becomes sufficiently small.[6] Accordingly, highly dispersed $BaTiO_3$ powders appear to be in the paraelectric cubic polymorphic form at room temperature, in contrast to the ferroelectric tetragonal form of bulk $BaTiO_3$.

The surface properties of $BaTiO_3$ crystals have been previously investigated both theoretically[7] and experimentally.[8] These works are of interest also in relation to its applicability as an anode for the photoelectrolysis of water[9] as well as to its potential use in heterogeneous catalysis[10] and photocatalysis[11] and in gas-sensor technology.[12]

The present paper summarizes our results on a bulk and surface chemical characterization of fine $BaTiO_3$ particles obtained by an hydrothermal method. The aim of this work is 2-fold: (i) to have information on the solid-state behavior of this high-area preparation; (ii) to have information on the surface chemical character of $BaTiO_3$ after and before previous calcination, in relation to possible surface-related applications and to the surface behavior of other mixed oxides.

Experimental Section

The hydrothermal preparation procedure of the $BaTiO_3$ powders has been described in detail elsewhere.[13] The method is based on the reaction between $Ba(OH)_2 \cdot H_2O$ and $TiCl_4$ (Aldrich, 99%) in NaOH (Fluka, 99%) aqueous solution. The reaction is carried out under atmospheric pressure at 358 K for 6 h. An excess of NaOH, as referred to the stoichiometric amount needed to neutralize HCl arising from $TiCl_4$ hydrolysis, is required to keep the pH value higher than 13 in order to exceed $BaTiO_3$ solubility and to allow its precipitation. After washing and drying, the powder shows to TEM analysis primary almost spherical particles with $\phi \leq 0.03$ μm with a certain degree of agglomeration ($\phi \leq 0.2$ μm). The BET surface area of the uncalcined sample is 39.5 m^2/g and drops to 7 m^2/g for the powder calcined at 1223 K for 15 h.

The FT-IR spectra have been recorded using a Nicolet Magna 750 Fourier transform instruments. For the region 5000–350 cm^{-1} a KBr beam splitter has been used with a DTGS detector,

† Università.
‡ CNR.
® Abstract published in *Advance ACS Abstracts,* June 1, 1994.

(1) West, A. R. *Solid State Chemistry and Its Applications*; Wiley: New York, 1984.
(2) Feinberg, J.; Heiman, D.; Tanguay, A. R.; Hellwarth, R. W. *J. Appl. Phys.* **1980**, *51*, 1297.
(3) Huybrechts, B.; Ishizaki, K.; Takata, M. *J. Am. Ceram. Soc.* **1992**, *75*, 722.
(4) Horn, R. G. *J. Am. Ceram. Soc.* **1990**, *73*, 1117.
(5) Hennings, D. In *Surface and Near-Surface Chemistry of Oxide Materials*; Nowotny, J., Defour, L. C., Eds.; Elsevier: Amsterdam, 1988; p 479.
(6) Niepce, J. C. In *Surfaces and Interfaces of Ceramic Materials*; Defour, L. C., et al., Eds.; Kluwer: Dordrecht, 1989; p 521.
(7) Wolfram, T.; Hurst, R.; Morin, F. J. *Phys. Rev. B* **1977**, *15*, 1151.
(8) Cord, B.; Courths, R. *Surf. Sci.* **1985**, *152/153*, 1141.
(9) Kennedy, J. H.; Frese, K. W. *J. Electrochem. Soc.* **1976**, *123*, 1683.
(10) Tejuca, L. G.; Fierro, J. L. G.; Tascon, J. M. D. *Adv. Catal.* **1989**, *36*, 237.
(11) Van Damme, H.; Hall, W. K. *J. Catal.* **1981**, *69*, 371.
(12) Arai, H.; Shimizu, Y. In *Chemical Sensor Technology*; Kondasha: Tokyo, 1989; p 83.
(13) Nanni, P.; Leoni, M.; Buscaglia, V.; Aliprandi, G. *J. Eur. Ceram. Soc.*, in press.

0897-4756/94/2806-0955$04.50/0

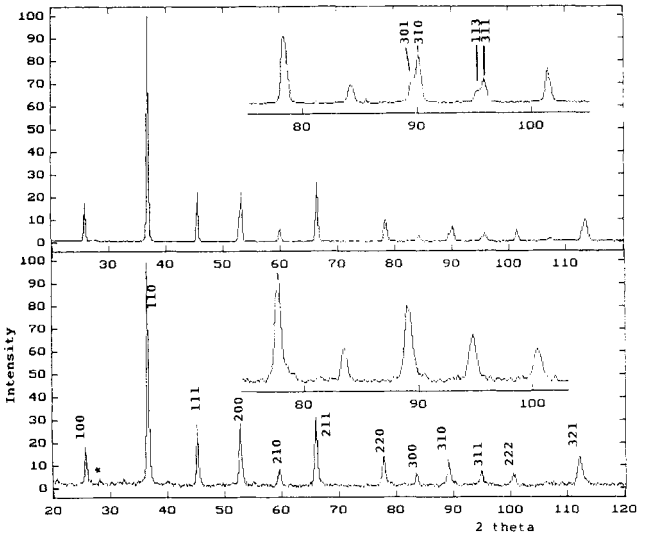

Figure 1. XRD patterns of $BaTiO_3$ as prepared (lower patterns) and after calcination at 1223 K for 15 h (upper patterns). The asterisk shows the main peak of $BaCO_3$.

while for the FIR region (600–50 cm^{-1}) a "solid substrate" beam splitter and a DTGS polyethylene detector have been used. For IR bulk characterization studies, different samples have been used, as pressed disks using KBr or polyethylene as binding materials or powders deposed on CsI monocrystals. For surface characterization studies the pure powder was pressed into self-supporting disks and was treated in conventional IR cells connected to outgassing/gas manipulation apparata.

The FT-Raman spectra have been recorded with a Bruker RFS100 instrument with a Nd:YAG laser (1061 nm), with laser power 30 mW, 50 scans, and resolution 4 cm^{-1}. XRD patterns have been recorded with a Philips PW 1710 system (Co Kα radiation). TEM analysis has been performed with Siemens Elmiskop 102 microscope.

Results and Discussion

(a) Bulk Characterization by Vibrational Spectroscopies. In Figure 1 the XRD patterns of the sample as prepared and after calcination at 1223 K for 15 h are compared. The XRD pattern of the sample as such corresponds to that of a cubic form of $BaTiO_3$ (JCPDS Table 31-174). The cell parameter we measure, $a = 0.4036(3)$ nm, corresponds to that reported by Naka[14] for this cubic phase ($a = 0.4031$ nm) but is significantly expanded with respect to the literature value for the cubic polymorph stable in the interval 393–1733 K ($a = 0.3996$ nm[15]). A negligible trace of $BaCO_3$ is also observed. After calcination at 1223 K the pattern is modified, with the splitting of some diffraction peaks. These splittings provide evidence for the deformation of the unit cell of $BaTiO_3$ from cubic to tetragonal (JCPDS Table 5-0626). The measured cell parameters ($a = 0.399(2)$, $b = 0.403(2)$ nm) correspond well to those reported in the literature ($a = 0.39920$, $b = 0.40361$ nm[15]) for tetragonal $BaTiO_3$.

The behavior of our preparation, as it appears to XRD analysis, is different from that of monocrystals and bulk materials, for which at least five different phases are stabilized at different temperatures. In the interval 393–1733 K $BaTiO_3$ monocrystals take the paraelectric "cubic perovskite" structure (space group $Pm3m = O_h^1$) with one formula unit per unit cell. Only below the Curie point near 393 K does $BaTiO_3$ become ferroelectric, with the tetragonal perovskite structure (space group $P4mm = C_{4v}^1$) with one formula unit per unit cell. This structure is obtained from the cubic structure with small shifts of titanium and oxygen ions along the c direction toward opposite sides.

The behavior of our sample is similar to that shown by other sol–gel-type preparations showing a cubic phase stable at room temperature.[14,16–22] Calcination to 1223 K allows to convert this material into powders with usual behavior, i.e., with the tetragonal phase stable at room temperature. However, this behavior will be checked on the basis of lattice vibrational data.

In fact, the O_h factor group analysis for a cubic perovskite brings to the following irreducible representation for the 12 fundamental optical modes:

$$\Gamma_{opt} = 3F_{1u}(\text{IR active}) + 1F_{2u}(\text{inactive})$$

So, a cubic perovskite does not show first-order Raman activity, being only the three triply degenerate IR-active modes expected. This has been confirmed for $SrTiO_3$ monocrystals, which are cubic at room temperature, for which Raman-active fundamentals can be detected only in the presence of an electric field that deforms the structure.[23] We have confirmed this with cubic $SrTiO_3$ powder, whose Raman spectrum does not show any sufficiently strong Raman peak.

For tetragonal $BaTiO_3$ the factor group is C_{4v}: the lowered symmetry of the unit cell causes each of the three F_{1u} modes to split into $A_1 + E$, while the F_{2u} modes also splits, into $B_1 + E$. Consequently, the following irreducible representation is obtained for the fundamental optical modes of tetragonal $BaTiO_3$:

$$\Gamma_{opt} = 3A_1(\text{IR and Raman active}) + 4E(\text{IR and Raman active}) + B_1(\text{Raman active})$$

So, these phases can be distinguished in principle by vibrational spectroscopies. In fact for cubic $BaTiO_3$ three IR-active fundamentals are expected without any first-order Raman activity, while for tetragonal $BaTiO_3$ eight Raman active modes, seven of which are also IR active, are expected.

The FT-IR and the FT-Raman spectra of our $BaTiO_3$ sample as such and after calcination for 15 h at 1223 K are shown in Figures 2 and 3. The observed bands are summarized in Table 1. The IR spectra of both samples in KBr pressed disks (Figure 2) are composed of a main couple of strong bands in the region 800–200 cm^{-1}. In the case of the sample calcined at 1223 K the higher frequency band is observed at 520 cm^{-1} with a shoulder at 680 cm^{-1}, while the lower frequency band is observed just at 400 cm^{-1} with a shoulder near 440 cm^{-1}. This spectrum agrees

(14) Naka, S. *Bull. Chem. Soc. Jpn.* **1974**, *47*, 1168.
(15) Landolt-Bornstein, *Numerical Data and Functional Relationships in Science and Technology*; Part III, Vol. 3, p 51.
(16) Vivekanandan, R.; Philip, S.; Kutty, T. R. N. *Mater. Res. Bull.* **1986**, *22*, 99.
(17) Dawson, W. J. *Am. Ceram. Soc. Bull.* **1988**, *67*, 1617.
(18) Vivekanandan, R.; Kutty, T. R. N. *Ceram. Int.* **1988**, *14*, 207.
(19) Hayashi, M.; Ishizawa, N.; Yoo, S. E.; Yoshimura, M. *J. Ceram. Soc. Jpn.* **1990**, *98*, 930.
(20) Kajiyoshi, K.; Ishizawa, N.; Yoshimura, M. *J. Am. Ceram. Soc.* **1991**, *74*, 369.
(21) Hennings, D.; Rosenstein, G.; Schreinemacher, H. *J. Eur. Ceram. Soc.* **1991**, *8*, 107.
(22) Ichinose, N.; Ozaki, Y.; Kashu, S. *Superfine Particle Technology*; Springer-Verlag: London, 1992; pp 140–142.
(23) Fleury, P. A.; Worlock, J. M. *Phys. Rev.* **1968**, *174*, 613.

Table 1. Position (cm^{-1}) of the Vibrational Bands Detected in $BaTiO_3$ Preparations[a]

cubic $BaTiO_3$ as prepared			tetragonal $BaTiO_3$			
CsI disk IR	bulk outg. IR	bulk in air Raman	CsI disk IR	bulk outg. IR	bulk in air Raman	assignments
4035						νOH+δOH int. OH
	3720			3720		νOH surface OH
	3680			3680		νOH surface OH
3503	3477	3523		(3480)		νOH internal OH
	2890					νCH impurity
	2824					νCH impurity
2452	2452					$\nu_{as}+\nu_s$ $BaCO_3$
1752	1752					$\nu_s+\delta_{ip}$ $BaCO_3$
1480				1440		ν_{as}C=O surf. CO_3^{2-}
1423			1420	(1420)		ν_{as}C=O $BaCO_3$
1365				1390		ν_{as}C=O surf. CO_3^{2-}
1060	1060	1060				ν_sC=O $BaCO_3$
857						δ_{oop} $BaCO_3$
692						δ_{ip} $BaCO_3$
650		707	680		713	lattice modes $BaTiO_3$
535		523	520		518	
413			440			
325			400		305	
		272			255	
		180			184	

[a] |: obscured regions (see text). ν = stretching modes; δ = deformation modes; s = symmetric; as = antisymmetric; ip = in-plane; oop = out-of-plane.

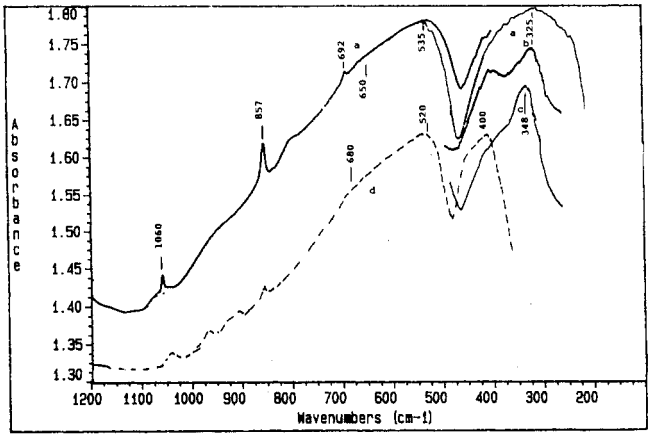

Figure 2. Skeletal FT-IR spectra of samples of $BaTiO_3$ powder: (a) as such KBr pressed disk; (b) powder deposed on a CsI monocrystal disk; (c) polyethylene pressed disk; (d) after calcination 15 h at 1223 K, KBr pressed disk.

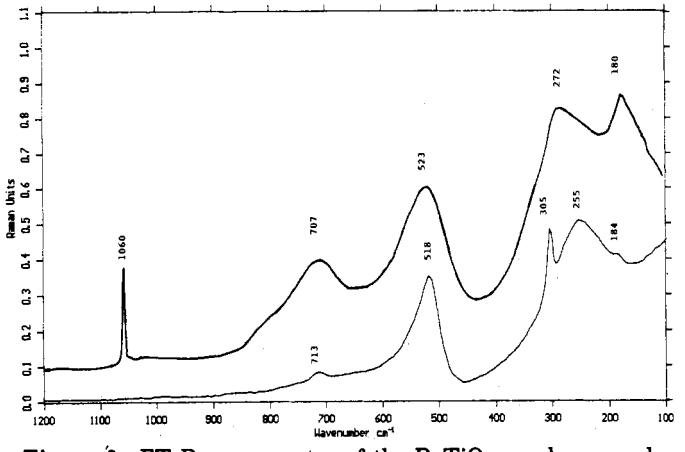

Figure 3. FT Raman spectra of the $BaTiO_3$ powder as such (top) and after calcination 15 h at 1223 K (bottom).

with the IR spectrum of tetragonal $BaTiO_3$ powders reported by several authors, that is somewhat variable, in relation to the particle size, shape, and aggregation.[24] The higher frequency band is reported by several authors in the region 560–520 cm^{-1} while the lower one shifts from 430 to 340 cm^{-1}.[24-28] An additional weak band is reported at 180 cm^{-1}.[24,26]

In the case of the uncalcined sample the higher frequency band is centered at 535 cm^{-1} with a shoulder near 650 cm^{-1}, while the shape of the lower frequency band strongly depends on the sample preparation and binding material. When the powder is passed in for KBr disks, this band appears broad and componentless with a maximum near 325 cm^{-1}, while when it is deposed on CsI we observe two components at 413 and 325 cm^{-1}, the latter being slightly stronger than the former. Finally, if the powder is pressed in polyethylene the maximum is at 340 cm^{-1}, with a higher frequency shoulder at 395 cm^{-1}.

So, the spectra we observe for both $BaTiO_3$ samples are similar to each other, despite some band shifts, and agree with literature data for tetragonal $BaTiO_3$, showing three bands at most. However, for tetragonal $BaTiO_3$ seven active modes are expected theoretically, while only three for the cubic phase. Nevertheless, Diaz Guemez et al.[24] discussed the IR spectrum of tetragonal $BaTiO_3$ powders on the basis of the cubic structure, assuming that "the deviation from an optically isotropic crystal can be neglected". This implies that the splitting of the three IR-active F_{1u} modes of cubic perovskite into A_1 + E is negligible (i.e., the three IR bands for tetragonal $BaTiO_3$ are each constituted by unresolved doublets) and that the new E IR-active component arising from the inactive F_{2u} mode of cubic perovskite remains too weak to be detected. So, unlike theory, the IR spectra in practice do not allow us to distinguish between cubic and tetragonal $BaTiO_3$.

The Raman spectrum of our tetragonal $BaTiO_3$ powder, previously calcined at 1223 K, shows a weak peak at 713 cm^{-1}, strong broad peaks at 518 and 255 cm^{-1}, a sharp peak at 304 cm^{-1}, and a pronounced shoulder at 184 cm^{-1}. The Raman spectrum of the uncalcined sample presents

(24) Diaz Guemes, M. I.; Gonzalez Carreno, T.; Serna, C. J. *Spectrochim. Acta* **1989**, *45A*, 589.
(25) Last, J. T. *Phys. Rev.* **1957**, *105*, 1740.
(26) Luxon, J. T.; Montgomery, D. J.; Summitt, R. *J. Appl. Phys.* **1970**, *41*, 2303.
(27) Dupuis, T.; Lorenzelli, V. *C.R. Acad. Sci. Paris, Ser. B* **1967**, *264*, 1019.
(28) Samuneva, B.; Jambazov, S.; Lepkova, D.; Dimitriev, Y. *Ceram. Int.* **1990**, *16*, 355.

some similarity with the previous one but with relevant differences: in the region 1000–100 cm^{-1} four strong maxima are detected at 707, 523, 272, and 180 cm^{-1}, with one evident shoulder near 800 cm^{-1}. The sharp peak at 1060 cm^{-1} is due to $BaCO_3$ impurities, as discussed below.

The Raman spectrum reported in Figure 3 for tetragonal $BaTiO_3$ closely agrees with those reported in the literature for tetragonal $BaTiO_3$ powders[29,30] and shows peaks nearly coincident with those of fundamental modes detected by Raman spectroscopy of tetragonal $BaTiO_3$ monocrystals.[31-33] Rimai et al.[31] and Chaves et al.[33] assigned peaks at 528, 280, and 170 cm^{-1} (not far from our bands at 518, 255, and 184 cm^{-1}) to the fundamental TO modes of A_1 symmetry, the peak at 305 cm^{-1} to the B_1 mode, while the E symmetry modes are either poorly split with respect to the A_1 modes (505 and 174 cm^{-1}) or fall below our detection range (10 cm^{-1}). The weak peak we observe at 713 cm^{-1} is almost coincident with the highest frequency longitudinal optical mode (LO) with A_1 symmetry.

The appearance of strong Raman peaks coinciding with fundamental TO modes of the tetragonal phase in the $BaTiO_3$ sample as prepared, in spite of the lack of detection of the B_1 mode near 305 cm^{-1} (probably not resolved from that at 255 cm^{-1}, appearing together at 275 cm^{-1}) definitely contrasts the cubic symmetry of the powder as deduced by XRD analysis, for which no first-order Raman activity is expected, and suggests a significantly lower symmetry with respect to a cubic perovskite structure, similar to that of tetragonal $BaTiO_3$.

A similar inconsistency of XRD and Raman analyses is sometimes observed in the case of mixed oxides. As a related example, we can cite the paper by Treiber and Kemmler-Sack[34] concerning some $A_3BM_2O_9$ perovskites, such as, for example, $Ba_3ZnNb_2O_9$. The XRD patterns of some of these compounds at low temperature are those expected for a cubic perovskite (space group $Pm3m = O_h^1$, with $^1/_3$ formula unit per cell), interpreted as evidence of a random distribution of Zn^{2+} and Nb^{5+} ions. However, Raman spectra contradict this information because of the appearance of strong peaks, likely associated with partial cation ordering. A very similar apparent disagreement of XRD and Raman techniques was recently observed by some of us in the case of the compound $FeCrO_3$.[35]

These apparent contradictions can arise from the microscopic nature of vibrational spectroscopy in contrast to the longer range order necessary to have a given X-ray diffraction pattern. According to other authors,[6,20] only when particle size raises a threshold value does the tetragonal structure of $BaTiO_3$ appear. Below this crystal size value the TiO_6 octahedra are probably still deformed, according to our Raman spectral data, but no sufficient tridimensional order exists in the bulk for appearance of the tetragonal distortion. In our case, the crystal size is strongly enhanced by calcination, from $\phi \leq 20$ nm to $\phi =$ 60 nm, according to TEM and XRD analyses.

According to Urban et al.,[29] the Raman spectrum of $BaTiO_3$ is also indicative of the Ba/Ti stoichiometry. In fact, according to these authors, when this stoichiometry is just one, the intensity of the peak at 713 cm^{-1} (measured with respect to that at 518 cm^{-1}) takes a minimum, while it grows when either Ba or Ti is in excess. The chemical analysis of our sample gives a ratio Ti:Ba+Sr = 1.04 (with 4.7% Sr natural impurity with respect to Ba), and this agrees with the weakness of the 713-cm^{-1} peak. The much higher relative intensity of the peak near 710 cm^{-1} in the Raman spectrum of the uncalcined sample with respect to the calcined one could be related to a much higher Ba-defect nonstoichiometry in the former, due to Ba segregation as $BaCO_3$ (see below).

(b) Vibrational Impurities Characterization. At higher frequencies with respect to the lattice region, additional components are observed in both IR and Raman spectra of our $BaTiO_3$ powder (Figures 2–5), as summarized in Table 1. The IR spectrum of the uncalcined sample (Figure 4a) shows a prominent band at 1423 cm^{-1} with shoulders both at its higher frequency side (near 1480 cm^{-1}) and at its lower frequency side (1365 cm^{-1}). Moreover very sharp bands can be observed at 2452, 1752, 1060, 857, and 692 cm^{-1}. The three bands at 1423, 857, and 692 cm^{-1} correspond to the three IR-active fundamentals (the asymmetric stretching, the out-of-plane deformation and the in-plane deformation) of a nearly symmetric carbonate ion, while the band at 1060 cm^{-1} corresponds to the symmetric stretching that is expected to be Raman active only for a symmetric CO_3^{2-} ion (D_{3h} point group) but can gain IR activity if the carbonate ion is less symmetric. Correspondingly, the Raman spectrum shows a very sharp intense peak just at 1060 cm^{-1}. The IR bands at 2452 and 1752 cm^{-1} are due to two combination modes of the same carbonate species. These absorptions correspond quite well with those reported for $BaCO_3$[36] and observed by us with a pure $BaCO_3$ sample. XRD shows negligible traces of $BaCO_3$ (Figure 1). The shoulders at 1480 and 1365 cm^{-1} indicate that also a different type of carbonate species exists, probably adsorbed on the surface and with lower symmetry evidenced by the splitting of the asymmetric stretching mode.

Additionally, both the IR and the Raman spectrum of the uncalcined sample show a feature near 3500 cm^{-1}. This feature is weak at 3523 cm^{-1} in the Raman spectrum, while it is reasonably strong centered at 3505 cm^{-1} in the IR spectrum and shows a weaker absorption at its higher frequency side (4035 cm^{-1}, insert in Figure 4). The main peak is certainly due to the stretching mode of OH groups present in the bulk. This will be further discussed below. The band near 4035 cm^{-1} should be due to a combination of the OH stretching mode at 3505 cm^{-1} with a lower frequency mode. This lower frequency mode could be reasonably an OH deformation mode, that is consequently expected near 530 cm^{-1}. However, it is not excluded that the OH stretching can combine with the $BaTiO_3$ fundamental mode we observe by IR spectroscopy at 540 cm^{-1}.

The IR and Raman analysis show that calcination at 1223 K for 15 h causes the substantial decrease of the bands associated to $BaCO_3$ impurities (Figure 4b). The IR spectra also show the almost complete disappearance

(29) Urban, M. W.; Cornilsen, B. C. In *Advances in Materials Characterization II*; Snyder, R. L., et al., Eds.; Plenum: New York, 1985; p 89.
(30) Javadpour, J.; Eror, N. G. *J. Am. Ceram. Soc.* **1988**, *71*, 206–213.
(31) Rimai, L.; Pasons, J. L.; Hickmott, J. T.; Nakamura, T. *Phys. Rev.* **1968**, *168*, 623.
(32) DiDomenico, M.; Wemple, S. H.; Porto, S. P. S.; Bauman, R. P. *Phys. Rev.* **1968**, *174*, 522.
(33) Chaves, A.; Katiyan, R. S.; Porto, S. P. S. *Phys. Rev.* **1974**, *B10*, 3522.
(34) Treiber, U.; Kemmler-Sack, S. *J. Solid State Chem.* **1982**, *43*, 51.
(35) Baraton, M. I.; Busca, G.; Prieto, M. C.; Ricchiardi, G.; Sanchez Escribano, V. *J. Solid State Chem.*, in press.
(36) Griffith, W. P. *J. Chem. Soc. A* **1970**, 286.

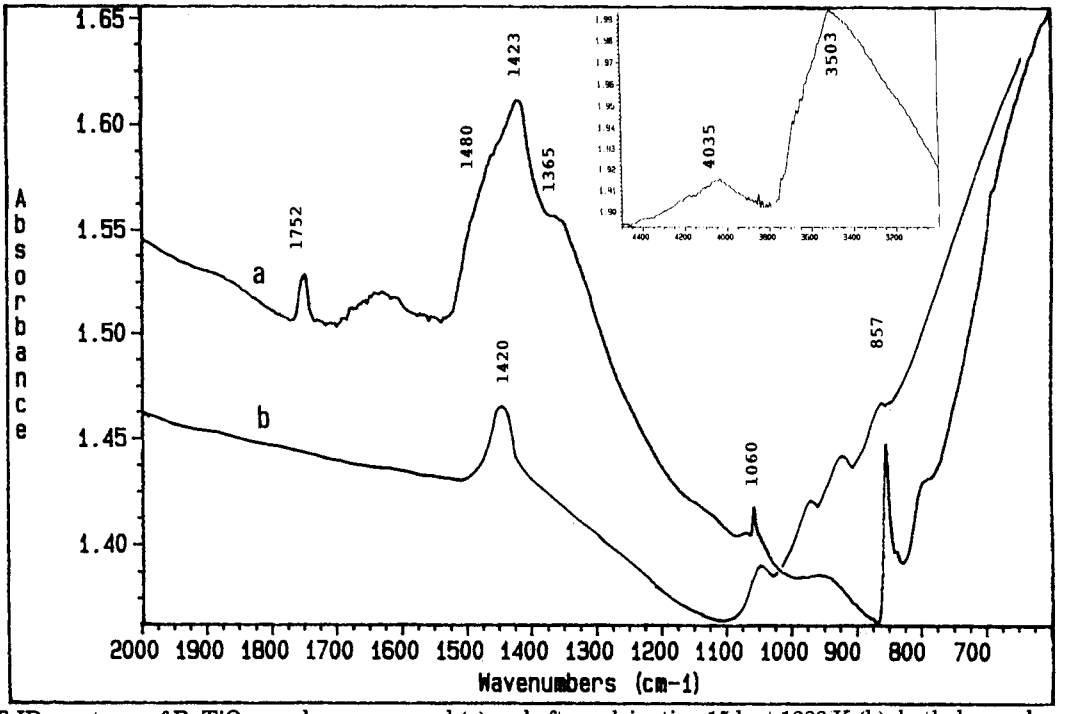

Figure 4. FT-IR spectrum of $BaTiO_3$ powder as prepared (a) and after calcination 15 h at 1223 K (b), both deposed on a CsI pressed disk (2000–600-cm^{-1} regions). In the insert, the region 4500–3000 cm^{-1} of $BaTiO_3$ as prepared powder deposed on a CsI pressed disk.

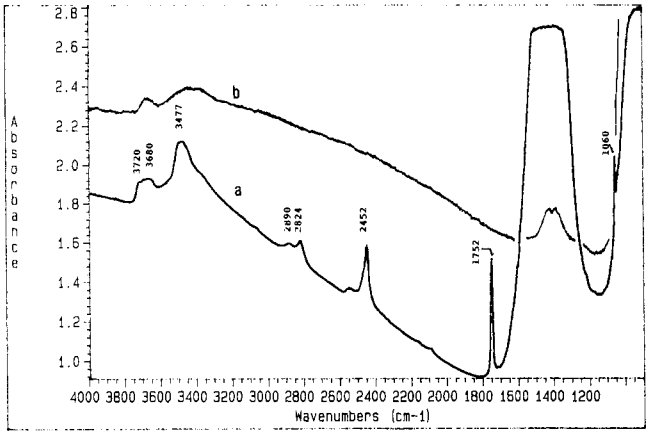

Figure 5. FT-IR spectrum of pressed disks of pure $BaTiO_3$ powder as such (a) and after calcination 15 h at 1223 K (b), both after outgassing at 673 K.

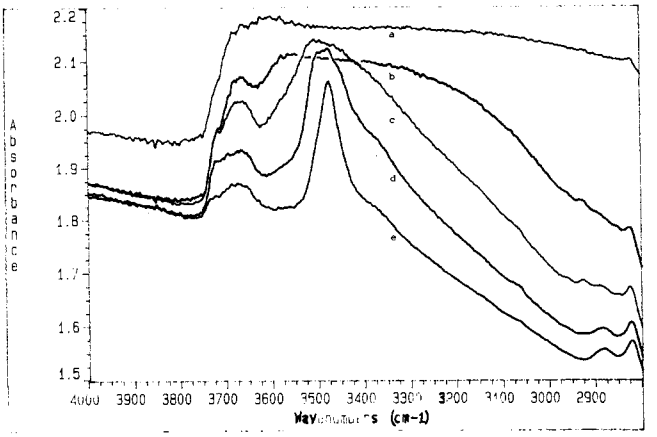

Figure 6. FT-IR spectra of a pressed disk of the pure $BaTiO_3$ powder as such, after outgassing at increasing temperatures: (a) 373, (b) 473, (c) 573, (d) 673, and (e) 773 K.

of the band due to internal OH's. The Raman spectrum does not allow to confirm the last conclusion, because of the development upon calcination of strong thermoluminescence effect in the 4000–2000-cm^{-1} region. The detection of internal OH's on hydrothermal cubic $BaTiO_3$ and their disappearance upon calcination was already cited by Vivekanandan and Kutty[16] although based on an OH deformation band, we do not observe.

(c) Surface Characterization. The FT-IR spectrum of a pressed disk of the pure uncalcined $BaTiO_3$ powder outgassed at 673 K is shown in Figure 5a. The sample transmits the IR radiation above 1520 cm^{-1} and between 1340 and 980 cm^{-1}. Below this cutoff limit the light is absorbed by the skeletal vibrational modes discussed above, while between 1520 and 1340 cm^{-1} the absorption is due to the asymmetric stretching of the carbonate ion impurities ($BaCO_3$), whose maximum is observed at 1423 cm^{-1} in KBr pressed disks (see above). Accordingly, this spectrum shows again the sharp bands at 1060, 1752, and 2452 cm^{-1}, already assigned to carbonate species, as well as sharp weak bands at 2890 and 2824 cm^{-1} due to C–H stretching of C-containing impurity species (possibly formate ions). These impurity absorptions have almost disappeared in the sample calcined at 1223 K (Figure 5b).

Above 1800 cm^{-1} the baseline grows as usual, because of the wavelength dependence of light scattering. The high transparency of the pressed disks of both powders above 1520 cm^{-1} provides evidence for the small particle size and for the absence of (semi)conductivity phenomena.

In the region 3800–3000 cm^{-1} the bands due to OH stretchings are observed as strong in the spectrum of the uncalcined sample but much weaker for the calcined one. Outgassing in the temperature range 300–773 K causes the decrease and the modification of the shape of these bands (Figure 6) due to water desorption and partial dehydroxylation. We can distinguish a weak broadish band at higher frequency, with a sharper component near 3720 cm^{-1} and a broader one centered at 3680 cm^{-1}. These absorptions are also present in the spectrum of the calcined sample (Figure 5b). This is the typical region for the

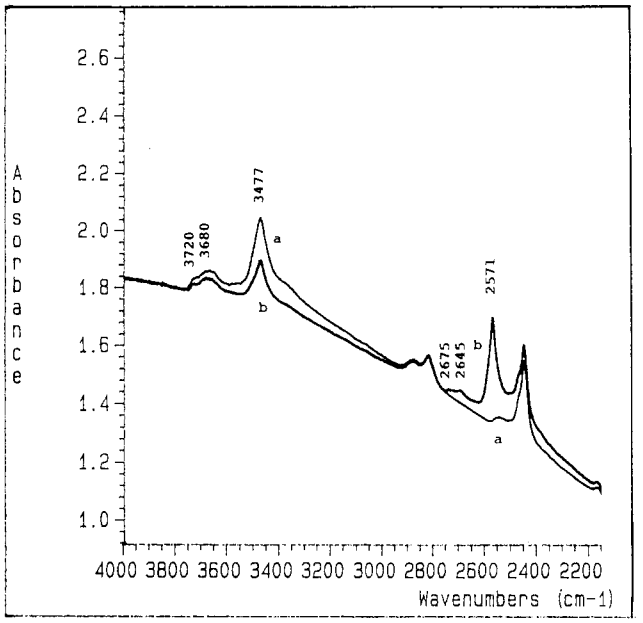

Figure 7. Effect of treating with D_2O vapor (10 Torr) at 473 K on the spectrum of $BaTiO_3$ pressed disk: (a) sample outgassed at 673 K; (b) sample exchanged with D_2O 10 Torr at 473 K for 2 h and outgassed at 673 K.

surface OH groups on metal oxides, and, in particular, on anatase and rutile TiO_2[37,38] as well as on alkaline-earth metal oxides.[38]

At lower frequencies a strong sharp band is observed only in the case of the uncalcined sample at 3477 cm^{-1} that could have a component at both its higher and lower frequency side. This band, that is definitely unusual on both binary and ternary metal oxides,[38,39] corresponds to the band observed at 3505 cm^{-1} in the IR spectrum of the powder deposed on CsI disks, as well as in the Raman spectrum too, as mentioned above. This band corresponds also to that observed just near 3480 cm^{-1} in $BaTiO_3$ monocrystals[40-43] and assigned to bulk hydrogen impurities. It is well-known that hydrogen impurities can penetrate several ternary oxides with perovskite structure[44,45] as H^+ bonded to a lattice oxygen in the form of an OH^-. These protons can compensate for the cation charge defect due either to reduced centers such as Ti^{3+} (or trivalent dopants) or to cation vacancies in nonstoichiometric samples.

Both surface and bulk OH's are at least partially exchangeable by heating at 475 K the $BaTiO_3$ pressed disk in D_2O vapor, as shown in Figure 7. This treatment causes the above-cited OH bands to decrease in intensity, while new bands grow at 2675 cm^{-1} (sharp and weak), 2645 cm^{-1} (broad and weak), and 2571 cm^{-1} (sharp and intense), due to the corresponding OD groups. The relatively easy exchange of bulk hydroxy groups confirms that the uncalcined $BaTiO_3$ perovskite structure is rather permeable to H^+ ions, as known for monocrystals.

To have an idea of the surface acidity of our $BaTiO_3$ preparations, we tested it using pyridine as an adsorbed probe molecule on disks previously outgassed at 773 K. The spectra of adsorbed pyridine (Figure 8) on the surfaces of both $BaTiO_3$ preparations are similar and are typical of the molecule coordinated on relatively weak Lewis acid sites. This can be deduced by the position of the ν8a and ν1 modes that are sensitive to the strength of Lewis acid sites. They are observed at 1593 and 998 cm^{-1} in both cases, slightly although significantly shifted with respect to the liquid-phase values (1583 and 990 cm^{-1}). Note that the weak band at 1612 cm^{-1} is due to the ν1 + ν6a combination. This band cannot be assigned to the ν8a of a second adsorbed species, as it is demonstrated by its decrease under outgassing, parallel to that of the band at 1593 cm^{-1}. To have a comparison, we can note that the ν8a and ν1 modes are observed at 1612 and 1016 cm^{-1} when pyridine is adsorbed on pure TiO_2,[37,46] while the ν8a mode is quoted just at 1592 cm^{-1} when adsorbed on CaO.[47] No data are reported on pyridine adsorption on BaO to our knowledge, although we observed a spectrum similar to that of Figure 8 for pyridine adsorption on a Ba aluminate.[48] As is well-known, the shift upward of the ν8a and ν1 modes of coordinated pyridine provides a measure of the strength of the Lewis acidic adsorbing cation. So, the surface of both $BaTiO_3$ preparations is very weakly acidic, and their exposed cations active in adsorption resemble Ba^{2+} cations more than Ti^{4+} cations usually exposed on titanium oxides. We can tentatively propose that the surface of $BaTiO_3$ presents coordinatively unsaturated Ba cations, while unsaturated Ti cations are not exposed on the surface or their acidity is deeply weakened with respect to that observed on TiO_2 polymorphs. Cord and Courths[8] previously concluded from their photoemission study of $BaTiO_3$ that the (100) surface of this structure is the most stable one. However, the crystal can terminate with two different (100) faces, one containing only oxygen and barium and the other containing only oxygen and titanium. These authors assumed that the latter should predominate, while our data suggest that the former should be predominant.

Conclusions

The main conclusions can be summarized as follows:

(a) The hydrothermal method we applied produces high-area $BaTiO_3$ particles useful for surface characterization by IR.

(b) This material as such appears to be cubic to XRD analysis, but Raman spectroscopy evidences that unit-cell distortions activate fundamental modes in a similar way as in tetragonal $BaTiO_3$. However, this phase is metastable, because it converts by calcination at 1223 K into the stable tetragonal $BaTiO_3$ phase.

(c) Carbonate impurities associated with $BaCO_3$ are evident in the sample as such. They disappeared almost completely in the tetragonal powder.

(37) Busca, G.; Saussey, H.; Saur, O.; Lavalley, J. C.; Lorenzelli, V. *Appl. Catal.* **1985**, *14*, 245.
(38) Boehm, H. P.; Knozinger, H. In *Catalysis Science and Technology*; Anderson, J. R., Boudart, M., Eds.; Springer-Verlag: Berlin, 1983, Vol. 4, p 39.
(39) Busca, G.; Lorenzelli, V.; Ramis, G.; Willey, R. J. *Langmuir* **1993**, *9*, 1492.
(40) Waser, R. *J. Am. Ceram. Soc.* **1988**, *71*, 58.
(41) Laulicht, I.; Benguigui, L. *Solid State Commun.* **1979**, *32*, 771.
(42) Kapphan, S.; Weber, G. R. *Ferroelectrics* **1981**, *37*, 673.
(43) Jovanovic, A.; Wohlecke, M.; Khappan, S.; Maillard, A.; Godefroy, G. *J. Phys. Chem. Solids* **1989**, *50*, 623.
(44) Kapphan, S. E. In *Nonstoichiometric Compounds*; Catlow, C. R. A., Mackrodt, W. C., Eds.; The American Ceramic Society: Westerville, OH, 1987; *Advances in Ceramics*, Vol. 23, p 379.
(45) Baikov, Yu. M.; Shalkova, E. K. *J. Solid State Chem.* **1992**, *97*, 224.
(46) Rives Arnau, V. R. *Opt. Pura Apl.* **1983**, *16*, 61.
(47) Tretyakov, H. E.; Filimonov, V. N. *Kinet. Katal.* **1973**, *14*, 803.
(48) Busca, G., Cristiani, C., Fozzatti, S., and Groppi, G., submitted paper.

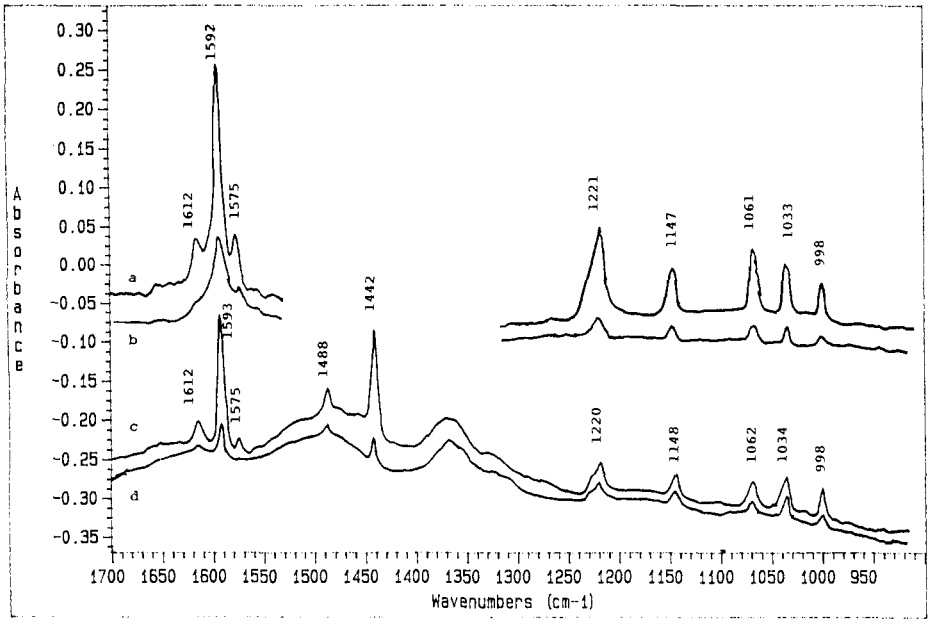

Figure 8. (a) FT-IR spectra of pyridine adsorbed on (a) uncalcined $BaTiO_3$ and evacuated at 300 K for 20 min; (b) the same after outgassing at 500 K for 5 min; (c) on $BaTiO_3$ (previously calcined at 1223 K) and evacuated at 300 K for 20 min; (d) the same after outgassing at 400 K for 5 min. The sample as prepared is opaque in the region 1520–1300 cm^{-1} (see text and Figure 5). The baseline in the region 1500–1300 cm^{-1} of the calcined sample is perturbed by the absorption of residual carbonates (see text and Figure 5).

(d) Bulk hydrogen impurities are also evident in the sample as such, in the form of hydroxy-groups as also occurs in tetragonal $BaTiO_3$ monocrystals, that are also stable in vacuum and readily isotopically exchangeable by D_2O. The observed vibrational frequencies (3477 cm^{-1} in vacuum) is almost the same as in tetragonal $BaTiO_3$ monocrystals. These hydrogen impurities, certainly present in large amounts, should be involved in the stabilization of the cubic form and disappear almost entirely by calcination at 1223 K.

(e) The surface related features we investigated (surface hydroxy groups and pyridine adsorption) are strictly analogous qualitatively for both the cubic metastable form and the stable tetragonal form.

(f) Surface hydroxy-groups are observable, absorbing in the region 3730–3650 cm^{-1}.

(g) Pyridine adsorption experiments show that the $BaTiO_3$ surface presents weak Lewis acidity, attributed to coordinatively unsaturated Ba^{2+} ions. This could be due to a predominance of the Ba–O-containing (100) faces, reported to be the most stable ones.

The last conclusion indicates that the basic nature of the BaO component predominates over the acidic nature of the TiO_2 component in the mixed oxide $BaTiO_3$. This contrasts with the conclusion obtained with another mixed oxide, the spinel $MgAl_2O_4$,[39] where the acidic nature of Al_2O_3 prevails over the basic nature of MgO. The study of surface acidity of other mixed oxides related to $BaTiO_3$ and $MgAl_2O_4$, such as Ba aluminates, titanates with the ilmenite structure such as $MgTiO_3$ and $NiTiO_3$, and other perovskite compounds, is now in progress in order to clarify the factors governing the predominance of the acidic or the basic component in mixed oxides (crystal structure type, stoichiometry, ionic radii, etc.).

The data reported above allow us to propose a mechanism explaining the "anomalous" solid-state behavior of this high-area $BaTiO_3$ powder, showing the XRD pattern of the cubic structure but a Raman spectrum associated with a lower symmetry. It seems reasonable to correlate this behavior with the presence of $BaCO_3$ impurities and of internal OH's in big amounts. We propose that, in the absence of sufficiently strong heat treatments, the perovskite structure remains very deficient in Ba, segregated as $BaCO_3$. This Ba deficiency in the perovskite structure is balanced by additional H^+, in the form of internal OH's, that give a sufficient elasticity to the structure to appear cubic to XRD analysis, despite the deformation of the TiO_6 octahedra evidenced by Raman spectroscopy. This leads to a metastable cubic form with a significant cell expansion with respect to the cubic perovskite form thermodynamically stable above 393 K. Calcination at sufficiently high temperatures allow further Ba to enter the structure, with the desorption of water and CO_2, and the actual composition approaches sufficiently the correct stoichiometry to assume the usual behavior, i.e., with the tetragonal ferroelectric form stable at room temperature.

Acknowledgment. Part of this work has been supported by MURST. The authors acknowledge Prof. P. Piaggio for the use of the FT Raman spectrometer.